

# HYPERREFLECTIVE RETINAL SPOTS IN NORMAL AND DIABETIC EYES

## B-Scan and En Face Spectral Domain Optical Coherence Tomography Evaluation

STELA VUJOSEVIC, MD, PhD,\* SILVIA BINI, MD,\* TOMMASO TORRESIN, MD,\*  
MARIANNA BERTON, MD,\* GIULIA MIDENA, MD,† RAFFAELE PARROZZANI, MD, PhD,\*  
FERDINANDO MARTINI, MD,\* PORZIA PUCCI, MD,\* ANNA R. DANIELE, MD,\*  
FABIANO CAVARZERAN, ScD,\* EDOARDO MIDENA, MD, PhD\*‡

---

**Purpose:** To evaluate hyperreflective retinal spots (HRS), in normal subjects and diabetic patients without and with macular edema (diabetic macular edema, DME), on linear B-scans and corresponding en face image of spectral-domain optical coherence tomography.

**Methods:** Retrospective evaluation of images of 54 eyes/subjects (16 normal subjects, 19 diabetic patients without DME, and 19 with DME). On horizontal B-scan spectral-domain optical coherence tomography, passing through the center of the fovea, the following characteristics of HRS were evaluated: location (inner retina or outer retina), size ( $\leq 30$  or  $> 30 \mu\text{m}$ ), reflectivity (similar to nerve fiber layer or to retinal pigment epithelium–Bruch complex), and presence or absence of back shadowing. On en face spectral-domain optical coherence tomography, the following patterns were evaluated: 1) isolated HRS (not corresponding to any visible lesion); 2) HRS corresponding to a segment of retinal capillary or microaneurysm wall; and 3) HRS corresponding to hard exudate. All gradings were performed twice by two graders in a masked fashion.

**Results:** Size  $\leq 30 \mu\text{m}$ , reflectivity similar to nerve fiber layer, and absence of back shadowing were associated with absence of vessels or any other lesion on en face image ( $P = 0.0001$  for all). Size  $> 30 \mu\text{m}$ , reflectivity similar to retinal pigment epithelium–Bruch complex, presence of back shadowing, and location in the outer retina were all associated with presence of hard exudate on en face imaging ( $P < 0.0001$  for all). Multiple logistic regression analysis showed that HRS present in the inner retina ( $P < 0.0001$ ), size  $> 30 \mu\text{m}$  ( $P = 0.0029$ ), and presence of back shadowing ( $P < 0.0001$ ) are directly associated with presence of microaneurysms on en face image. Intragrader and intergrader repeatability were excellent for all evaluations.

**Conclusion:** Hyperreflective retinal spots  $\leq 30 \mu\text{m}$ , reflectivity similar to nerve fiber layer, and absence of back shadowing may represent activated microglial cells; HRS  $> 30 \mu\text{m}$ , reflectivity similar to retinal pigment epithelium–Bruch complex, presence of back shadowing, and location in the outer retina may represent hard exudate; HRS  $> 30 \mu\text{m}$ , presence of back shadowing, and location in the inner retina may represent microaneurysms. These hypotheses may be tested in further studies.

**RETINA** 0:1–12, 2016

---

Hyperreflective retinal spots (HRS) have been recently described in different chorioretinal vascular and degenerative disorders.<sup>1–8</sup> Hyperreflective retinal spots are described as small, sometimes punctiform, reflective lesions, visible on spectral-domain optical coherence tomography (SD-OCT) B-scans, in both inner retina (IR) and outer retina (OR).<sup>1–8</sup>

In eyes with macular edema because of diabetic retinopathy (DR), retinal vein occlusion, or age-related macular degeneration (AMD), HRS were described also near the retinal cysts or even in the walls or inside the lumen of the cysts in the OR.<sup>1,2,4,7</sup> Recent histologic evidence from human donor eyes with AMD and acquired vitelliform lesions shows that

anteriorly migrated retinal pigment epithelium (RPE) cells (up to the outer plexiform layer [OPL]) are also visualized as HRS on SD-OCT and are often associated with external limiting membrane and/or ellipsoid zone disruptions.<sup>9–11</sup> Moreover, in neovascular AMD, hyperreflective foci (spots) can be both RPE and lipid filled cells (thought to be microglia), predicting that HRS had at least two cellular origins that could be discerned via multimodal imaging.<sup>10</sup> In normal subjects, HRS were mostly described in the IR layers.<sup>6</sup> Although there are an increasing number of published articles on the evaluation of HRS on SD-OCT, there is still no consensus on their origin, location, characteristics, and significance. The most common hypotheses include biomarker of inflammation (activated and aggregated microglial cells); (precursors of) hard exudates (HEs); and degenerated photoreceptor cells, anteriorly migrated RPE cells, and retinal vessels (including microaneurysms, etc).<sup>1–11</sup> Thus, very different interpretation and possible implication for disease management could be assigned to HRS. Moreover, there is no available data on reproducibility of HRS quantification, limiting the validity of its quantification, especially in clinical practice. With the advent of en face SD-OCT, a coronal view of the macula, at different depths, can be obtained, thus adding more detailed information on topographic location and lateral extent of any specific lesion, and correlation of OCT data to other imaging modalities.<sup>12,13</sup>

The main purpose of this study was to evaluate in detail specific characteristics of HRS in normal subjects and diabetic patients without and with macular edema (diabetic macular edema, DME) on linear B-scans (SD-OCT) and corresponding en face imaging to better understand HRS significance. The secondary aim was to evaluate intragrader and intergrader agreements in the quantification of HRS to validate their evaluation.

## Materials and Methods

### Population

This is a retrospective evaluation of images of 54 eyes/subjects (16 normal subjects, 19 diabetic pa-

tients without macular edema, and 19 with DME). All patients had slit-lamp biomicroscopy examination, fundus color photography (Topcon, TRC 50IA; Topcon, Tokyo, Japan), SD-OCT (Spectralis HRA+OCT; Heidelberg Engineering, Heidelberg, Germany), with the acquisition of en face images. To be eligible for this grading study, the patients had to have all imaging modalities of reasonably good quality obtained on the same day. The main exclusion criteria were as follows: myopia >6 diopters, significant media opacity, any previous macular treatment (laser treatment and or intravitreal injections), and proliferative DR. Normal eyes (nondiabetic) had no signs of any retinal or choroidal disease.

Informed consent was obtained from each patient, and the research was carried out in accordance with the Declaration of Helsinki. Local Ethics Committee approval for the study was obtained.

### *Spectral-Domain Optical Coherence Tomography: En Face and B-Scan*

En face imaging is a novel imaging technique derived from SD-OCT, which gives transverse coronal scans (called “C-scans”) of the retina and choroid. For the purpose of this study, all en face OCT images were obtained with a single diagnostic system (Spectralis HRA+OCT; Heidelberg Engineering), which uses a superluminescence diode at 870 nm wavelength. The scanning protocol of the retina used the following parameters: 20° × 20° volume scans centered on the fovea, 5.8 mm<sup>2</sup> (range, 5.7–5.9 mm), 50 frames automatic linear time, 97 horizontal sections, 60 μm apart. B-scans (conventional line scan SD-OCT) are derived from sagittal and transverse sections. Each OCT B-scan had resolution of 512 A-scan with high-speed mode.

### *Image Grading*

Hyperreflective spots (HRS) were evaluated on a B-scan, which was displayed at 200% magnification on a monitor simultaneously with and below an en face map. The HRS were evaluated between 500 μm and 1,500 μm temporally from the center of the fovea on the horizontal linear scan passing through the center of the fovea.<sup>6,14</sup> The grading area was delimited using a transparent sheet, on which 2 vertical markers were traced at the measured distances (500 μm and 1,500 μm) (Figure 1). Hyperreflective retinal spots, defined as small, punctiform, and isolated reflective lesions/dots, were evaluated in the IR (defined as all layers between the inner limiting membrane and the OPL) and in the OR (defined as the Henle nerve fiber layer [NFL] and outer nuclear

From the \*Department of Ophthalmology, University of Padova, Padova, Italy; †University Campus Biomedico, Roma, Italy; and ‡Fondazione G. B. Bietti, IRCCS, Roma, Italy.

Supported by, as GB Bietti Foundation is concerned, the Ministry of Health and Fondazione Roma. This study was mainly supported by the grant from the 7th Frame-work Programme (EUROCONDOR. FP7-278040).

None of the authors have any conflicting interests to disclose.

Reprint requests: Edoardo Midena, MD, PhD, Department of Ophthalmology, University of Padova, Via Giustiniani 2, Padova 35128, Italy; e-mail: edoardo.midena@unipd.it

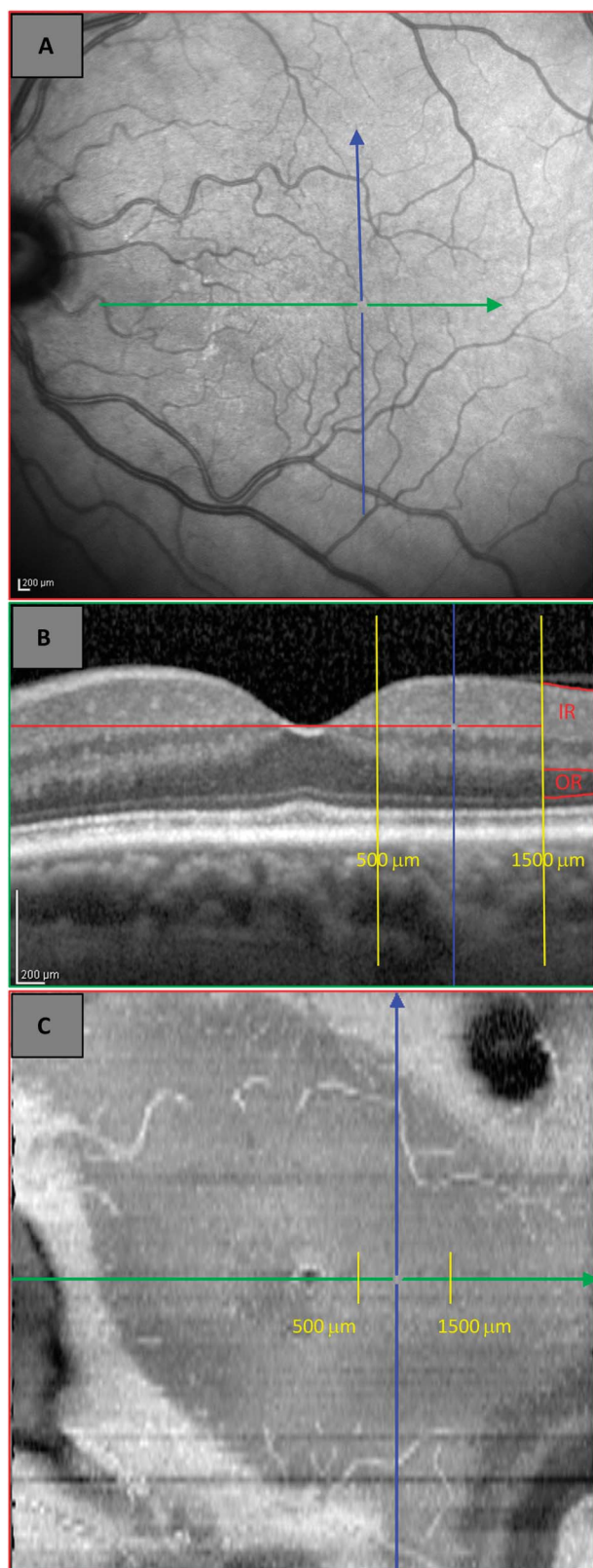


**Fig. 1.** Infrared fundus image (A), OCT B-scan (B), and en face OCT image (C) of the left eye of normal subject (nondiabetic) showing the area temporal to the fovea where HRS were evaluated (delimited with 2 vertical markers traced at distances of 500  $\mu\text{m}$  and 1,500  $\mu\text{m}$ ). The

layer).<sup>15</sup> For each hyperreflective spot, the following parameters were evaluated on B-scan: location (IR or OR; and when intraretinal cysts were present [in DME eyes], also location in respect to the cysts), size ( $\leq 30 \mu\text{m}$  or  $> 30 \mu\text{m}$ , considering the largest diameter of the HRS), presence or absence of back shadowing, and reflectivity (2 levels of hyperreflectivity were identified: moderate reflectivity similar to normal NFL and high reflectivity similar to RPE–Bruch membrane complex [RPE–Bruch complex]).<sup>15</sup> After defining these parameters, the cursor was positioned on each HRS on the linear B-scan at 0° displayed below the en face map. The sliding of the cursor to the exact position of the HRS on linear B-scan allows the identification of the corresponding image on en face map (also in the three-dimensional image). Thus, HRS were first identified on the 0° linear B-scan and then compared with their corresponding image on the en face map. The position of HRS identified on the en face image was also compared with infrared image underlying the same en face image/map (Figures 1 and 2). The use of en face image modality was mostly important when evaluating HRS corresponding to the presence of small retinal vessels and microaneurysms not always easily seen on B-scan OCT image (Figures 3 and 4). Correlation was assessed between HRS detected on linear B-scan and following patterns on en face image: 1) isolated hyperreflective spot (not corresponding to any visible lesion); 2) HRS corresponding to a segment of retinal capillary or microaneurysm wall; and 3) HRS corresponding to HE. The presence of microaneurysms or HE was confirmed by the comparison with fundus color image.

All gradings were performed twice (for intragrader agreement) by two independent graders (intergrader agreement) in a masked fashion to each other gradings and to clinical data of patients.

### Statistics

Intragrader and intergrader agreements were both evaluated by intraclass correlation coefficient (ICC

intersection point (which exactly corresponds to the same point on all three images is obtained automatically by the instrument) shows no visible lesion on infrared image; IR is defined as all layers between the inner limiting membrane and the OPL; OR is defined as the Henle NFL and outer nuclear layer. Hyperreflective retinal spots located in the IR (characterized by small dimension, reflectivity similar to NFL, not forming any back shadowing) as visible on B-scan; and isolated hyperreflective spot on en face image. The intersection point of blue and green arrow on A and C and blue and red on B, (which exactly corresponds to the same point on all 3 images is obtained automatically by the instrument) shows no visible lesion on infrared image (A), and shows isolated HRS on B and C.

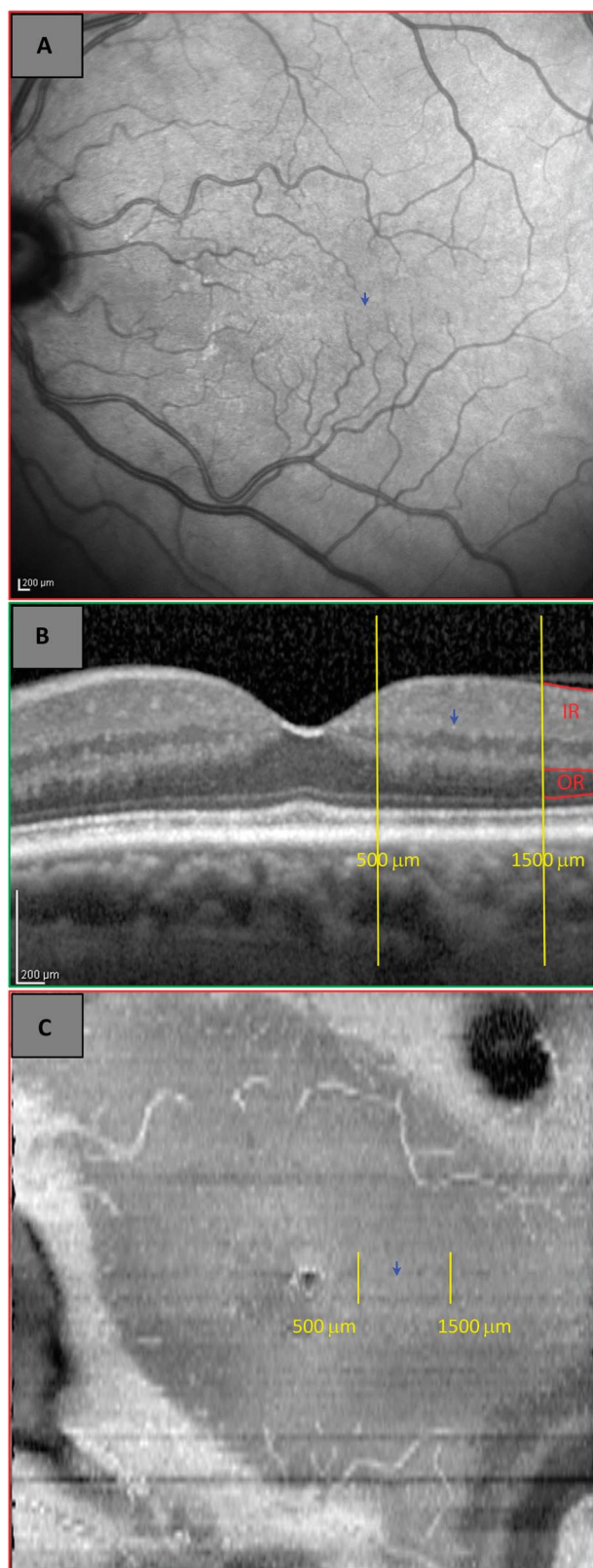


**Fig. 2.** Infrared fundus image (A), OCT B-scan (B), and en face OCT image (C) of the same left eye as in Figure 1 but without overlays. A normal subject (nondiabetic) shows the area temporal to the fovea where HRS were evaluated (delimited with 2 vertical markers traced at

(2,1)) and Bland–Altman plots (Figure 5). For the analysis of intragrader agreement, two evaluations of each grader were used, whereas for intergrader agreement, only the first evaluation of each grader was used. For statistical analyses, only results of Grader 1 were used.

To investigate the association between HRS characteristics on linear B-scan and en face SD-OCT map, two types of statistical analyses were performed. Univariate Fisher exact test was applied to frequency tables of en face outcome (three categories) for each HRS characteristic. In addition, multiple logistic regression analysis was performed with “no lesion” (en face outcome) as reference group. For this analysis, eyes with HE were excluded from the sample because they were observed only in DME group and “quasi-separation” of cases could imply infinity estimates of model’s parameters. Explanatory variables included in the model were coded as follows: location = 1 if IR, 0 if OR; dimension = 1 if  $>30\ \mu\text{m}$ , 0 if  $\leq 30\ \mu\text{m}$ ; reflectivity = 1 if similar to RPE–Bruch complex, 0 if similar to NFL; back shadowing = 1 if present, 0 if absent; only in case of DME, location of HRS was evaluated with respect to cysts: 1 if HRS was intracystic, 0 if HRS was along the cyst’s wall perimeter.

## Results

Fifty-four eyes of 54 subjects (16 normal subjects, 19 diabetic patients without clinical signs of maculopathy, and 19 with DME) were evaluated by 2 graders. All diabetic patients had diabetes mellitus Type 2. Mean age was  $68.1 \pm 4.5$  years for normal subjects;  $67.8 \pm 5.6$  years for diabetic patients with DR and without DME; and  $65.4 \pm 2.5$  years for diabetic patients with DME. All 19 eyes without DME had mild or moderate DR, with no HEs or hemorrhages in the macula. Patients with DME had moderate DR. Mean central retinal thickness was  $471.2 \pm 101.9\ \mu\text{m}$  in DME eyes.

A total of 944 HRS were counted by Grader 1 and 891 by Grader 2. Table 1 shows the frequencies of different characteristics of HRS evaluated by the 2 graders, on both B-scan and en face SD-OCT, in all 3 examined groups.

distances of  $500\ \mu\text{m}$  and  $1,500\ \mu\text{m}$ ). Inner retina is defined as all layers between the inner limiting membrane and the OPL. Outer retina is defined as the Henle NFL and outer nuclear layer. Blue arrow indicates the HRS evaluated at the intersection point (refer Figure 1) located in the IR (characterized by small dimension, reflectivity similar to NFL, not forming any back shadowing) as visible on B-scan and isolated hyperreflective spot on en face image; on infrared image, blue arrow indicates no visible lesion.

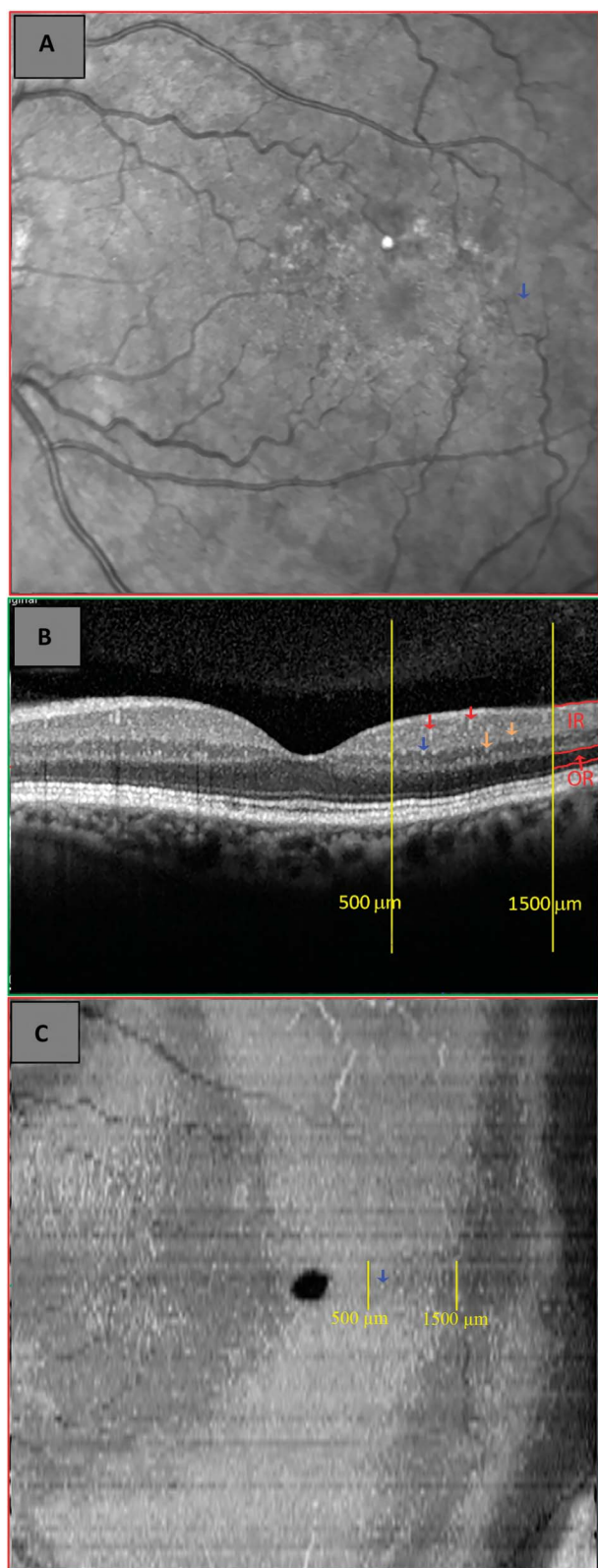


**Fig. 3.** Infrared fundus image (A), OCT B-scan (B), and en face OCT image (C) of the left eye of a diabetic patient without macular edema (no-DME) showing the area temporal to the fovea where HRS were evaluated (delimited with 2 vertical markers traced at distances of

Table 2 shows the association between parameters evaluated on linear B-scan and on en face OCT images. Univariate analysis shows highly significant association between parameters evaluated on B-scan and specific en face lesion ( $P < 0.0001$ ). For example: location in the IR,  $\leq 30 \mu\text{m}$  size, reflectivity similar to NFL, and absence of back shadowing were associated with isolated hyperreflective spot on en face OCT image (not corresponding to vessels or any other visible lesion) ( $P < 0.0001$  for all) (Table 2). Hyperreflective retinal spots with these characteristics were always present in the IR (in 100% of eyes) in all 3 groups of patients (normal subjects, patients with DME, and patients without DME). Location in the OR,  $>30 \mu\text{m}$  in size, reflectivity similar to RPE–Bruch complex, and presence of back shadowing were all associated with presence of HE on en face image ( $P < 0.0001$  for all) (Table 2). In patients with DME, when HRS location was evaluated, in relation to cysts, in almost all cases, HRS were located along the wall of the cysts (Table 2 and Figure 4). Multiple logistic regression analysis shows that HRS in the IR ( $P < 0.0001$ ), size  $>30 \mu\text{m}$  ( $P = 0.0029$ ), and presence of back shadowing ( $P < 0.0001$ ) is directly associated with the presence of microaneurysms on en face image (Table 2). Reflectivity similar to NFL was equally associated with no visible lesion and with microaneurysms on en face image ( $P = 0.1727$ ; Table 2).

Table 3 shows more in detail different characteristics of HRS corresponding to isolated HRS on en face image (thus to absence of vessels or any other visible lesion) in the 3 different groups of patients (normal subjects, patients with DME, and patients without DME). Hyperreflective retinal spots with these characteristics were always present in the IR in all three groups of patients (in normal eyes only in the IR). When total number of HRS was evaluated, distribution between IR and OR showed that the number of HRS in the OR was significantly higher in DME eyes (approximately 25% of HRS,  $P < 0.0001$ ) than in normal (0% of HRS in the OR) and no-DME eyes (approximately

500  $\mu\text{m}$  and 1,500  $\mu\text{m}$ ). Inner retina is defined as all layers between the inner limiting membrane and the OPL. Outer retina is defined as the Henle NFL and outer nuclear layer. Blue arrows indicate the intersection point (refer Figure 1), which exactly corresponds to the same point on all 3 images and is obtained automatically by the instrument, showing: no visible lesion on infrared image; HRS located in the IR (characterized by small dimension, reflectivity similar to NFL, not forming any back shadowing) as visible on B-scan; and an isolated HRS on en face image. On B-scan: orange arrows indicate HRS with same characteristics as the one indicated with blue arrow (corresponding to microglial cells), and red arrows indicate HRS with dimension  $>30 \mu\text{m}$ , reflectivity similar to NFL with back shadowing corresponding to retinal capillaries from superficial vascular network.

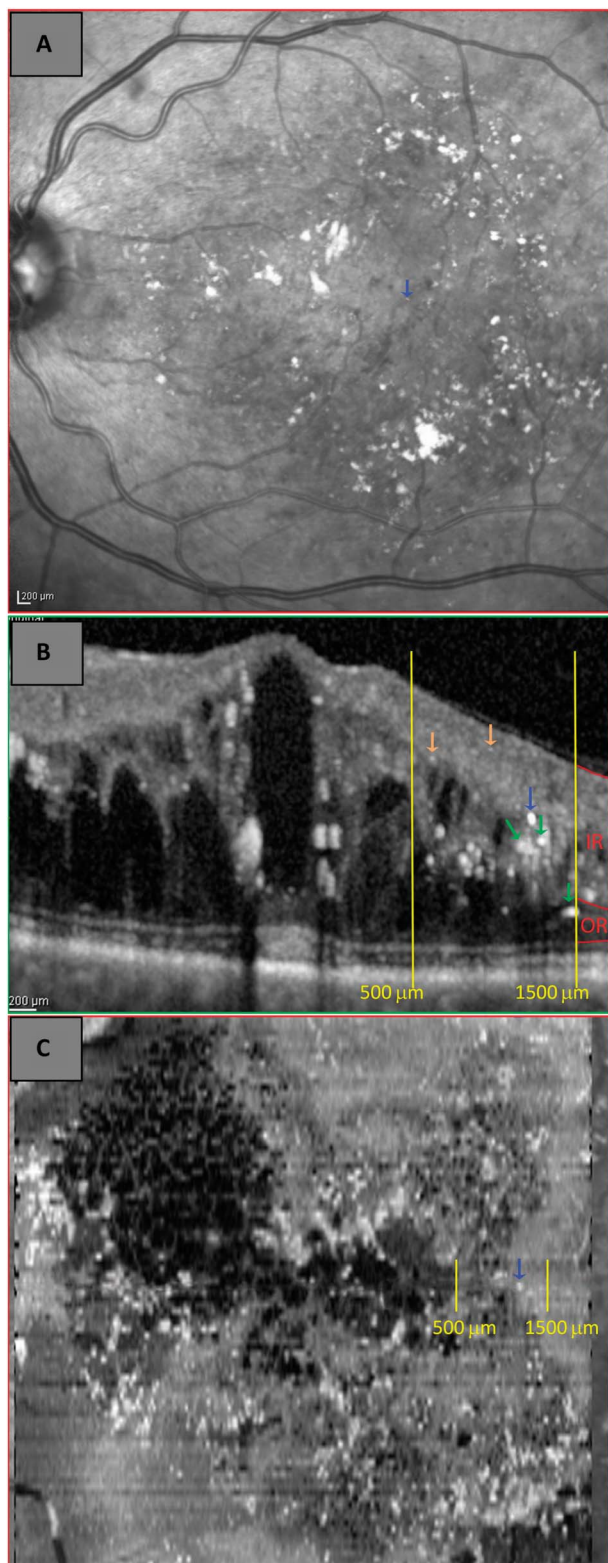


**Fig. 4.** Infrared fundus image (A), OCT B-scan (B), and en face OCT image (C) of the left eye of a diabetic patient with exudative macular edema (DME) showing the area temporal to the fovea, where HRS were evaluated (delimited with 2 vertical markers traced at distances of 500  $\mu\text{m}$  and 1,500  $\mu\text{m}$ ). Inner retina is defined as all layers between the inner limiting membrane and the OPL. Outer retina is defined as the

15% of HRS) (Table 3). Hyperreflective retinal spots were mostly  $\leq 30 \mu\text{m}$  in size, reflectivity similar to NFL (all HRS in normal and no-DME eyes), whereas in DME eyes, 97.4% of HRS had size  $\leq 30 \mu\text{m}$  ( $P = 0.049$ ) and 95.4% of HRS had reflectivity similar to NFL ( $P = 0.0007$ ). Back shadowing was absent in almost all cases in all 3 groups (Table 3).

Table 4 shows data of intragrader and intergrader repeatability. Intragrader repeatability was excellent for all evaluations, for both B-scans SD-OCT and en face images: intraclass correlation coefficient at least 0.99 (95% confidence interval ranging from at least 0.98 to 0.99) (Table 4). Intergrader repeatability was excellent for all evaluations on B-scan and en face images: with intraclass correlation coefficient of at least 0.82 (95% confidence interval: 0.71–0.99).

Bland–Altman plots show no deviations from the expected pattern of intragrader and intergrader agreements: magnitude of bias (average discrepancy between measurements) resulted low and very close to 0 (almost all measurements between  $\pm 2$  SD); 95% limits of agreement resulted very narrow in comparison with the average of measurements. There is no trend, and the variability is consistent across the graphs in all 3 groups (Figure 5 for intergrader agreement; data not shown for intragrader agreement).

## Discussion

In this study, we report detailed information about HRS visible on linear B-scans (SD-OCT), and the correlation to specific lesions visible on corresponding en face SD-OCT image in normal subjects, diabetic patients without macular edema and diabetic patients with DME. Different parameters of HRS were evaluated: location (IR or OR), intracyst or along the cyst wall location (in case of DME with intraretinal cysts), size, reflectivity, and presence of back shadowing. The main reason to evaluate these specific characteristics is to try to obtain more precise information on HRS in normal subjects and in

Henle NFL and outer nuclear layer. Blue arrows indicate the intersection point (refer Figure 1), which exactly corresponds to the same point on all 3 images and is obtained automatically by the instrument, showing: small HE on infrared image; HRS located in the IR (reflectivity similar to REP–Bruch complex, forming back shadowing) as visible on B-scan; HE visible on en face image. On B-scan: green arrows indicate HRS of different dimensions corresponding to HE (with same reflectivity characteristics as the one indicated with blue arrow) (other larger HE are easily visualized on B-scan as HRS outside the delimited area of evaluation, with large dimensions, located in both inner and OR and within the wall of cysts with back shadowing). Orange arrows indicate small HRS in the IR with reflectivity similar to NFL without any back shadowing (corresponding to microglial cells).

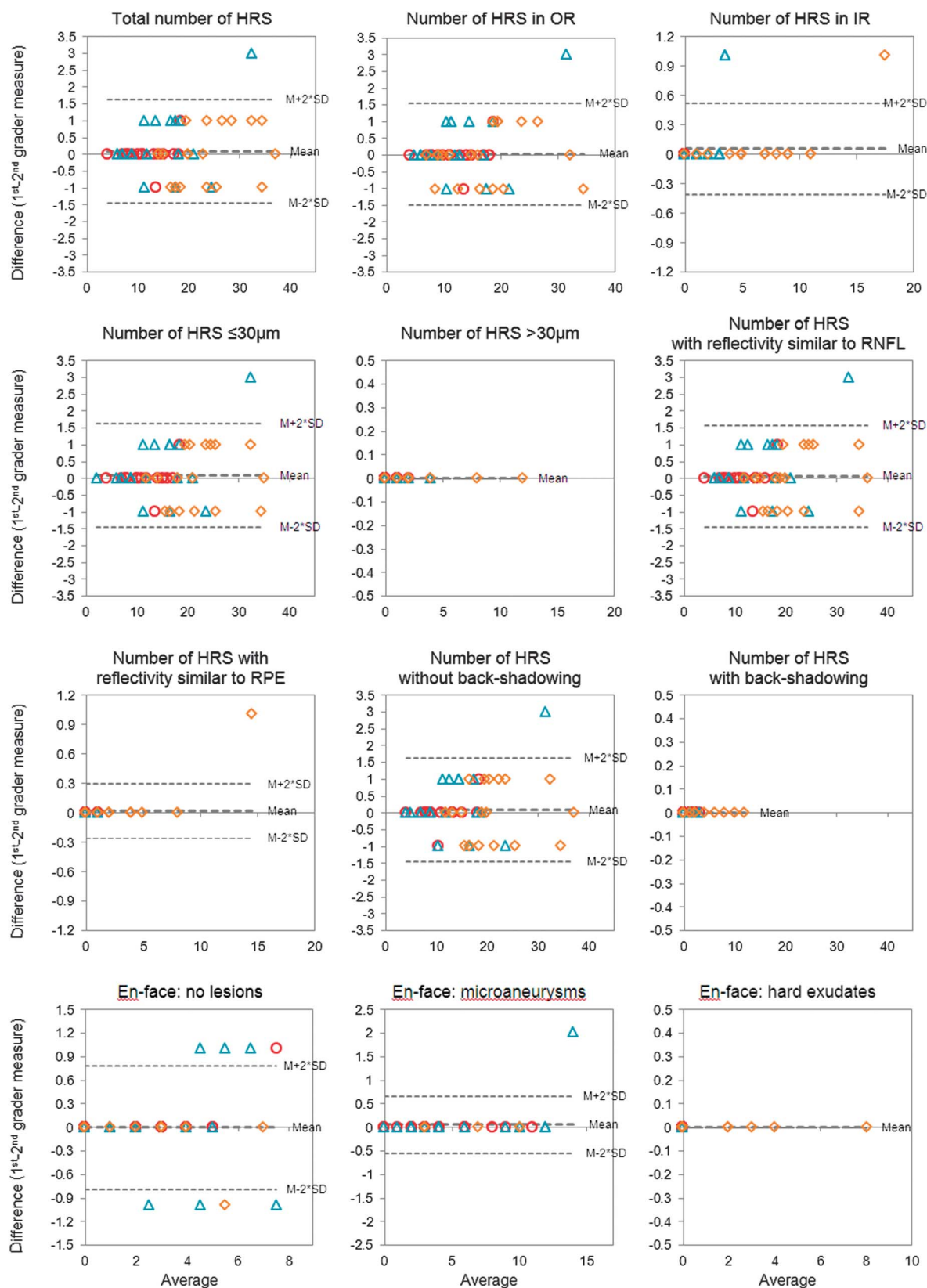


**Fig. 5.** Bland–Altman graphs. Bland–Altman plots of intergrader agreement in the three groups:  $\circ$ , normal subjects;  $\Delta$ , diabetic patients without ME (macular edema);  $\diamond$ , diabetic patients with ME showing almost all measurements between  $\pm 2SD$ s. RNFL, retinal nerve fiber layer.

Table 1. Different Characteristics of HRS Evaluated by Two Independent Graders in Normal Subjects, Diabetic Patients Without Macular Edema and Diabetic Patients With Macular Edema (Number of HRS in the First and Second Evaluations)

Characteristic	Grader 1								Grader 2							
	Subjects								Subjects							
	Normal		Diabetic Patients w/o ME		Diabetic Patients With ME		Total		Normal		Diabetic Patients w/o ME		Diabetic Patients With ME		Total	
	1st	2nd	1st	2nd	1st	2nd	1st	2nd	1st	2nd	1st	2nd	1st	2nd	1st	2nd
Total	178	180	292	283	474	474	944	937	177	177	270	265	444	444	891	886
Location																
OR	0	0	28	29	113	114	141	143	0	0	24	22	117	116	141	138
IR	178	180	264	254	361	360	803	794	177	177	246	243	327	328	750	748
Location respect to cyst																
Within wall	0	0	0	0	97	98	97	98	0	0	0	0	94	94	94	94
Inside	0	0	0	0	4	4	4	4	0	0	0	0	2	2	2	2
Dimension, $\mu\text{m}$																
$\leq 30$	174	176	284	275	433	433	891	884	172	172	263	258	404	404	839	834
$> 30$	4	4	8	8	41	41	53	53	5	5	7	7	40	40	52	52
Reflectivity																
NFL	176	178	291	282	432	432	899	892	174	174	269	264	402	403	845	841
RPE–Bruch complex	2	2	1	1	42	42	45	45	3	3	1	1	42	41	46	45
Back shadowing																
No	165	167	276	267	429	429	870	863	165	165	254	249	395	395	814	809
Yes	13	13	16	16	45	45	74	74	12	12	16	16	49	49	77	77
En face																
No lesion	118	119	195	188	350	352	663	659	116	116	168	165	340	341	624	622
Vessel/microaneurysms	60	61	97	95	98	96	255	252	61	61	102	100	81	80	244	241
HEs	0	0	0	0	22	22	22	22	0	0	0	0	19	19	19	19

The term no lesion (under en face OCT classification) is an isolated hyperreflective spot on en face image not corresponding to any visible lesion on color image or infrared image.  
1st, first evaluation; 2nd, second evaluation; ME, macular edema; w/o, without.

Table 2. Association Between HRS Characteristics and En Face Classification

Characteristic	En Face Classification			<i>P</i> *	Microaneurysms Vs. No Lesions†	
	No Lesions	Vessel/Microaneurysms	Hard Exudates		Odds Ratio (95% CI)	<i>P</i> ‡
Location				<0.0001		
OR	115 (17.3)	5 (2.0)	21 (95.5)		1 (Ref)	
IR	548 (82.7)	250 (98.0)	1 (4.5)		18.5 (5.9–58.8)	<0.0001
Dimension, $\mu\text{m}$				<0.0001		
$\leq 30$	653 (98.5)	233 (91.4)	1 (4.5)		1 (Ref)	
$> 30$	10 (1.5)	22 (8.6)	21 (95.5)		6.3 (1.9–21.4)	0.0029
Reflectivity				<0.0001		
RPE–Bruch complex	16 (2.4)	7 (2.7)	20 (90.9)		1 (Ref)	
NFL	647 (97.6)	248 (97.3)	2 (9.1)		2.6 (0.7–10.2)	0.1727
Back shadowing				<0.0001		
Absent	650 (98.0)	217 (85.1)	3 (13.6)		1 (Ref)	
Present	13 (2.0)	38 (14.9)	19 (86.4)		9.0 (3.8–21.7)	<0.0001
Location respect to cyst§				<0.0001	n.a.	
Within wall	79 (98.7)	0 (0.0)	18 (100.0)			
Inside	1 (1.3)	3 (100.0)	0 (0.0)			

\*Univariate analysis (Fisher exact test).

†Vessel/microaneurysms versus no lesions (multiple logistic regression analysis).

‡Wald chi-square test.

§Patients with diabetic macular edema only.

CI, confidence interval; n.a., not applicable because of lack of cases.

diabetic eyes. In fact, there are different reports on HRS significance in macular diseases and normal subjects.<sup>1–11,14,16</sup> Coscas et al<sup>1</sup> were the first to describe small, punctiform hyperreflective elements, scattered throughout all retina layers, but mostly in the OR, in AMD. These authors interpreted HRS as activated microglial cells in late-stage AMD.<sup>1</sup> Lad et al<sup>17</sup> documented microglia involvement by immunohistochemistry in human autopsy eyes with late-

stage AMD (geographic atrophy and choroidal neovascularization). Madeira et al<sup>18</sup> reported microglial activation in different retinal degenerative diseases (including DR) contributing to chronic neuroinflammation, with release of proinflammatory mediators (by activated microglial cells), and increased oxidative stress and nitrosative stress.<sup>18,19</sup> These activated microglial cells could be visualized in the retina as HRS, by SD-OCT.<sup>1,6,10,14,18</sup> Vujosevic et al<sup>6</sup> reported

Table 3. Association Between HRS Characteristics Corresponding to Isolated HRS on En Face Image (No Visible Lesion on Infrared Image) and Different Subject Groups (N = 663)

Characteristic	Normal Subjects	Diabetic Patients w/o ME	Diabetic Patients With ME	<i>P</i> *
Location				<0.0001
OR	0 (0)	28 (14.4)	87 (24.9)	
IR	118 (100)	167 (85.6)	263 (75.1)	
Dimension, $\mu\text{m}$				0.049
$\leq 30$	117 (99.1)	195 (100.0)	341 (97.4)	
$> 30$	1 (0.9)	0 (0.0)	9 (2.6)	
Reflectivity				0.0007
RPE–Bruch complex	0 (0.0)	0 (0.0)	16 (4.6)	
NFL	118 (100.0)	195 (100.0)	334 (95.4)	
Back shadowing				0.0137
Absent	117 (99.1)	195 (100.0)	338 (96.6)	
Present	1 (0.9)	0 (0.0)	12 (3.4)	
Location respect to cyst†				n.a.
On the wall	0 (0.0)	0 (0.0)	79 (98.7)	
Inside	0 (0.0)	0 (0.0)	1 (1.3)	

All values are absolute number; values in parenthesis are expressed as percentage.

\*Univariate analysis (Fisher exact test).

†Patients with diabetic macular edema only.

ME, macular edema; w/o, without.

Table 4. Repeatability Analysis: Intraclass Correlation Coefficient, ICC(2,1)

Characteristic	Intragrader 1		Intragrader 2		Intergrader	
	ICC	95% CI	ICC	95% CI	ICC	95% CI
Total no. HRS	0.996	0.992–0.997	0.990	0.983–0.994	0.931	0.876–0.961
Location						
OR	0.998	0.997–0.999	0.994	0.990–0.997	0.994	0.905–0.967
IR	0.994	0.990–0.997	0.987	0.977–0.992	0.910	0.839–0.949
Location respect to cyst						
On the wall	1.000		0.996	0.994–0.998	0.938	0.896–0.964
Inside	1.000		1.000		0.797	0.673–0.877
Dimension, $\mu\text{m}$						
$\leq 30$	0.995	0.991–0.997	0.989	0.981–0.994	0.925	0.867–0.957
$> 30$	1.000		1.000		0.975	0.958–0.986
Reflectivity						
NFL	0.995	0.991–0.997	0.988	0.980–0.993	0.925	0.865–0.958
RPE–Bruch complex	0.998	0.997–0.999	1.000		0.989	0.980–0.993
Back shadowing						
No	0.995	0.991–0.997	0.989	0.980–0.993	0.917	0.851–0.953
Yes	1.000		1.000		0.974	0.955–0.985
En face						
No lesions	0.996	0.993–0.998	0.987	0.978–0.993	0.887	0.812–0.933
Microaneurysms	0.996	0.993–0.998	0.993	0.989–0.996	0.823	0.712–0.894
HEs	1.000		1.000		0.975	0.958–0.986

CI, confidence interval; ICC, intraclass correlation coefficient.

the increase in HRS in diabetic patients versus normal subjects (even in diabetic eyes without any clinical sign of retinopathy), suggesting that HRS may represent aggregates of activated microglial cells that migrate, with the progressing of the disease, from more IR layers to more OR layers, confirming previous histopathologic findings.

Other authors proposed that HRS in the OR in DME were closely associated with disrupted external limiting membrane and IS/OS line, suggesting their origin from degenerated photoreceptors or macrophages engulfing them.<sup>3</sup> Bolz et al<sup>2</sup> and Deák et al<sup>7</sup> hypothesized that hyperreflective foci (corresponding to HRS) may represent subclinical features of lipoprotein extravasation or lipid-filled macrophages that act as precursors and/or components of HE in diabetic patients with macular edema. In this study, we found that not all HRS, visible on SD-OCT linear scans are similar. In fact, HRS located in the OR, with larger size ( $>30 \mu\text{m}$ ), higher reflectivity (similar to RPE–Bruch complex), and with back shadowing are mostly associated with the presence of HE, visible on both en face image and confirmed on color fundus image. Deák et al<sup>7</sup> described HRS at the apical part of the outer nuclear layer in DME eyes, classifying them as microexudates, which after 4 months of follow-up formed conglomerates of HRS involving also OPL and inner nuclear layer, and were visible on color fundus photograph and infrared image as HE. Gelman et al<sup>20</sup> described the presence of so-called “pearl necklace sign” of HRS forming a contigu-

ous ring along the wall of cystoid spaces in the OPL in patients with chronic exudative maculopathies in different retinal vascular diseases. These authors found that these HRS are highly reflective (similar to RPE–Bruch complex) and large.<sup>20</sup> Also in the present study, patients with DME and visible HE had corresponding HRS located within the cysts wall, with reflectivity similar to RPE–Bruch complex, and larger size (Table 2).

Instead, HRS located mostly in the IR, dimension  $>30 \mu\text{m}$ , moderate reflectivity similar to NFL, and with back shadowing, were mostly associated with the presence of microaneurysms. In fact, recent studies using OCT angiography in the macula described and confirmed that retinal vascular networks in the macula are located in the NFL and ganglion cell layer (the superficial vascular network) and in the inner nuclear layer (deep vascular network).<sup>21,22</sup> The superficial vascular network is formed of vessels of approximately  $75 \mu\text{m}$  diameter, whereas the deep vascular network is formed by dense and complex system of smaller vessels of approximately  $20 \mu\text{m}$  diameter. These two networks are in communication through small vessels in vertical course.<sup>21,23</sup>

In contrast, HRS located always in the IR (in all cases) but also in the OR (mostly in DME eyes), small in size ( $\leq 30 \mu\text{m}$ ), with moderate reflectivity similar to NFL without any back shadowing were not correlated to any specific lesion visible on color fundus images. Moreover, these characteristics of HRS (located only in the IR and completely absent in the outer nuclear layer) were also present in normal subjects without any

clinical sign of retinopathy. Thus, HRS with these characteristics may represent aggregates of microglial cells. In fact, their location is in the IR in normal subjects, whereas in DME, they were also located in the OR (Table 3). Therefore, it can be assumed that HRS found in the OR, with above described characteristics, may be because of activated and migrated (aggregates of) microglial cells and not because of the presence of retinal capillaries, as these are not present within the Henle NFL and outer nuclear layer.

The higher number of total HRS in normal eyes found in this study, compared with our previously reported data,<sup>6</sup> is because of greater magnification of B-scan OCT images used in this study and probably better visualization of HRS corresponding to small retinal vessels located in the IR (Table 1).

The major limitations of this study include limited number of examined eyes and the fact that HRS present in the INL–OPL, size  $<30\ \mu\text{m}$ , and reflectivity similar to the NFL although not forming any back shadowing on B-scan OCT and not determining any visible lesion on en face OCT image cannot be completely excluded to be some small retinal capillaries. Therefore, a larger study, using other imaging modalities also, may be useful to precisely distinguish between some small capillaries in specific retinal layers and activated microglial cells in diabetic patients and other vascular diseases. Although HRS were evaluated between  $500\ \mu\text{m}$  and  $1,500\ \mu\text{m}$  from the fovea (mostly to include major number of microaneurysms and HE and vessels), Frizziero et al<sup>24</sup> recently showed that HRS can be also evaluated in the central  $500\text{--}\mu\text{m}$  area, even if fovea shows different anatomical characteristics, as lack of specific retinal layers.

Moreover, in this study, we documented that HRS evaluation is a reliable method, with high intragrader and intergrader agreement on SD-OCT images in either normal subjects without any signs of retinopathy or diabetic patients without macular edema and diabetic patients with DME. Although the presence of DME with large cysts and numerous HEs may influence OCT linear images evaluation, HRS may become a novel OCT parameter of retinal inflammatory process in diabetic patients to be evaluated in clinical practice and trials. Moreover, HEs, represented by HRS with specific characteristics, rarely can be interpreted as aggregates of activated microglial cells. This study may help to better characterize the hyperreflective spots/dots/foci and for future evaluation of inflammatory retinal response in vascular diseases.

**Key words:** hyperreflective spots, OCT, microglia, diabetic retinopathy, diabetic macular edema.

## References

1. Coscas G, De Benedetto U, Coscas F, et al. Hyperreflective dots: a new spectral-domain optical coherence tomography entity for follow-up and prognosis in exudative age-related macular degeneration. *Ophthalmologica* 2013;229:32–37.
2. Bolz M, Schmidt-Erfurth U, Deak G, et al. Optical coherence tomographic hyperreflective foci: a morphologic sign of lipid extravasation in diabetic macular edema. *Ophthalmology* 2009;116:914–920.
3. Uji A, Murakami T, Nishijima K, et al. Association between hyperreflective foci in the outer retina, status of photoreceptor layer, and visual acuity in diabetic macular edema. *Am J Ophthalmol* 2012;153:710–717, 717.e1.
4. Framme C, Schweizer P, Imesch M, et al. Behavior of SD-OCT-detected hyperreflective foci in the retina of anti-VEGF-treated patients with diabetic macular edema. *Invest Ophthalmol Vis Sci* 2012;53:5814–5818.
5. Ogino K, Murakami T, Tsujikawa A, et al. Characteristics of optical coherence tomographic hyperreflective foci in retinal vein occlusion. *Retina* 2012;32:77–85.
6. Vujosevic S, Bini S, Midena G, et al. Hyperreflective intraretinal spots in diabetics without and with nonproliferative diabetic retinopathy: an in vivo study using spectral domain OCT. *J Diabetes Res* 2013;2013:491835.
7. Deák GG, Bolz M, Kriechbaum K, et al; Diabetic Retinopathy Research Group Vienna. Effect of retinal photocoagulation on intraretinal lipid exudates in diabetic macular edema documented by optical coherence tomography. *Ophthalmology* 2010;117:773–779.
8. De Benedetto U, Sacconi R, Pierro L, et al. Optical coherence tomographic hyperreflective foci in early stages of diabetic retinopathy. *Retina* 2015;35:449–453.
9. Zanzottera EC, Messinger JD, Ach T, et al. The Project macula retinal pigment epithelium grading system for histology and optical coherence tomography in age-related macular degeneration. *Invest Ophthalmol Vis Sci* 2015;56:3253–3268.
10. Pang CE, Messinger JD, Zanzottera EC, et al. The onion sign in neovascular age-related macular degeneration represents cholesterol crystals. *Ophthalmology* 2015;122:2316–2326.
11. Chen KC, Jung JJ, Curcio CA, et al. Intraretinal hyperreflective foci in acquired vitelliform lesions of the macula: clinical and histologic study. *Am J Ophthalmol* 2016;164:89–98.
12. Sallo FB, Peto T, Egan C, et al; MacTel Study Group. “En face” OCT imaging of the IS/OS junction line in type 2 idiopathic macular telangiectasia. *Invest Ophthalmol Vis Sci* 2012;53:6145–6152.
13. Puche N, Querques G, Blanco-Garavito R, et al. En face enhanced depth imaging optical coherence tomography features in adult onset foveomacular vitelliform dystrophy. *Graefes Arch Clin Exp Ophthalmol* 2014;52:555–562.
14. Vujosevic S, Berton M, Bini S, et al. After anti-VEGF treatment in center-involving diabetic macular edema. *Retina* 2016;36:1298–1308.
15. Staurenghi G, Sadda S, Chakravarthy U, Spaide RF. International Nomenclature for Optical Coherence Tomography (IN•OCT) Panel. Proposed lexicon for anatomic landmarks in normal posterior segment spectral-domain optical coherence tomography: the IN•OCT consensus. *Ophthalmology* 2014;121:1572–1578.
16. Pemp B, Deák G, Prager S, et al; Diabetic Retinopathy Research Group Vienna. Distribution of intraretinal exudates in diabetic macular edema during anti-vascular endothelial

- growth factor therapy observed by spectral domain optical coherence tomography and fundus photography. *Retina* 2014;34:2407–2415.
17. Lad EM, Cousins SW, Van Arnam JS, Proia AD. Abundance of infiltrating CD163+ cells in the retina of postmortem eyes with dry and neovascular age-related macular degeneration. *Graefes Arch Clin Exp Ophthalmol* 2015;253:1941–1945.
  18. Madeira MH, Boia R, Santos PF, et al. Contribution of microglia-mediated neuroinflammation to retinal degenerative diseases. *Mediators Inflamm* 2015;2015:673090.
  19. Block ML, Hong JS. Microglia and inflammation-mediated neurodegeneration: multiple triggers with a common mechanism. *Prog Neurobiol* 2005;76:77–98.
  20. Gelman SK, Freund KB, Shah VP, Sarraf D. The pearl necklace sign: a novel spectral domain optical coherence tomography finding in exudative macular disease. *Retina* 2014;34:2088–2095.
  21. Savastano MC, Lumbroso B, Rispoli M. In vivo characterization of retinal vascularization morphology using optical coherence tomography angiography. *Retina* 2015;35:2196–2203.
  22. Spaide RF, Klancnik JM Jr., Cooney MJ. Retinal vascular layers imaged by fluorescein angiography and optical coherence tomography angiography. *JAMA Ophthalmol* 2015;133:45–50.
  23. Duke-Elder S. *The Anatomy of Visual System*. Vol 2. London, United Kingdom: C.V. Mosby Co; 1961:372–376.
  24. Frizziero L, Parrozzani R, Midena G, et al. Hyperreflective intraretinal spots in radiation macular edema on spectral domain optical coherence tomography. *Retina* 2016;36:1664–1669.